International Journal of Pharmaceutics 416 (2011) 260–267

Contents lists available at ScienceDirect

International Journal of Pharmaceutics

journal homepage: www.elsevier.com/locate/ijpharm

Development and characterization of a new thief sampling device for cohesive powders

L. Susana, P. Canu, A.C. Santomaso*

DIPIC-Department of Chemical Engineering Principles and Practice, University of Padova, via Marzolo 9, 35131 Padova, Italy

ARTICLE INFO

Article history:
Received 29 March 2011
Received in revised form 4 July 2011
Accepted 4 July 2011
Available online 13 July 2011

Keywords:
Powder sampling
Thief probe
Homogeneity assessment

ABSTRACT

New sampling probes and methods for investigating cohesive powders are conceived, designed and characterized. Probes are made of two metallic shells (a slide and a cover) which need to be inserted sequentially into the bed of powder in order to extract representative samples. The thin profile of the shells, combined with a particular insertion procedure, is intended to minimize stresses on the powder; thereby reducing both the invasiveness and the dragging of material through the bed. Probes of similar design with different shape and size have been tested on stratified beds of cohesive powders of different colors. Sampling performances are quantitatively compared among different probes (for size and shape) and also with literature data. The comparison has indicated that the new sampling devices effectively improved sampling efficiency, reliability and possibilities. The simple construction and use suggest they can be viable and effective alternatives to traditional probes for cohesive mixtures.

1. Introduction

The need for sampling a mixture of powders for analytical purposes naturally arises during intentional mixing or handling due to undesirable powder behavior, such as unwanted segregation. Mixing of powders is a common and critical unit operation in solids processing (Bridgwater, 1976; Harnby, 2000). Methods for precise characterization of powder mixtures must be available, both for routine process control and to sustain the development of predictive models, which will improve equipment design and planning mixing strategies (Santomaso et al., 2005). The purpose of sampling is to collect a predetermined quantity of powder (typically some grams), which is expected to be representative of the whole solid mixture under examination. It requires the highest level of accuracy to guarantee significance to the following quantitative analyses. Mixture characterization imply the quantitative assessment of both chemical (i.e. composition) and physical (e.g. particle size) homogeneity.

An effective mixing requires preventing or minimizing segregation. Free-flowing powders containing particles with different physical properties (particle size, density, shape) are known to segregate (Bridgwater, 1976; Zik et al., 1994; Santomaso et al., 2004). Specifically, any induced flow causes particles to move differently and to accumulate selectively into different regions of the mixer (Santomaso et al., 2004). Experience suggests that free-flowing dry powders with size larger than 75–100 μm are prone to segregate while reducing size below 75 μm minimizes segregation at large scale of scrutiny because of the increased cohesion (Harnby, 1992). However, while segregation maybe reduced with cohesive powders, it can still occur at a smaller scale because of the development of stable microstructures of small aggregates with composition different from the surrounding mixture. Depending on the nature and strength of interparticulate forces, agglomerates can dominate the flow characteristics and transform the cohesive mixture in a system of free-flowing aggregates (Harnby, 1992). Ultimately, both free-flowing and cohesive powders may experience segregation. Also ingredients in very low quantity jeopardize mixture homogeneity since there is a critical scale of scrutiny at which content uniformity of such ingredients can be excessively poor (Danckwerts, 1953). In every industrial activity where thorough mixture homogeneity is essential, such as pharmaceutical, reliable sampling and characterization methods of solid mixtures are critical operations. In this context, thief probes are traditionally used to sample bulk powders and check if products meet specifications.

However, traditional thief sampling techniques present some severe limitations (Muzzio et al., 1997). Alternative in-line analytical technologies have been developed such as light-induced fluorescence, light reflectance, effusivity and near-infrared spectroscopy (Benedetti et al., 2007), but thief sampling remains the routine procedure in many pharmaceutical companies to validate large scale powder mixing operations (Mendez et al., 2010). Representative sampling involves two distinct aspects: the distribution of sampling events both in space and time and the actual collection of material from the mixture. While the former issue is mainly a

* Corresponding author. Tel.: +39 049 8275491; fax: +39 049 8275461.
E-mail address: andrea.santomaso@unipd.it (A.C. Santomaso).

0378-5173/$ – see front matter © 2011 Elsevier B.V. All rights reserved.
doi:10.1016/j.ijpharm.2011.07.003

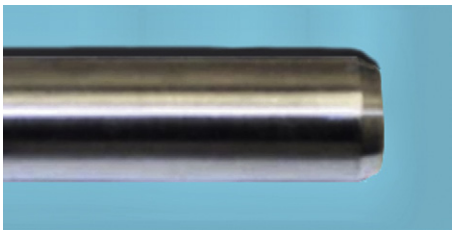

Fig. 1. Picture of a core sampler (CS).

statistical problem, already discussed by Muzzio et al. (1997) and considered in the Draft Guidance addressing the issue of unit sampling and assessment (U.S. Food and Drug Administration, 2003). The latter is fundamental to any further speculation and requires the availability of suitable probes and operating methods. Muzzio et al. (1999, 2003) thoroughly demonstrated that traditional thief probes used in the pharmaceutical industry may not yield representative samples of the actual mixing degree and proved that they are particularly invasive, since they modify the structure of the original bed of powder, thus biasing the collected sample.

Thief probes are typically made of two concentric cylinders, in which the inner cylinder has one or more cavities that can be opened and closed by rotating the outer one, which acts as the probe cover. This type of probe allows taking samples from the mixture when the holes of the outer cylinder are aligned with the cavities of the inner one. Thief probes are called *side-* or *end-sampling probes*, depending on the location of the cavities, i.e. several on the side or a single one at the lower extremity. In both cases, the probe is introduced into the powder bed with its cavities closed. Once insertion is complete, the rotation of the outer cylinder opens the cavities allowing the powder to flow inside. The cavities are then closed before withdrawal of the probe. The aforementioned published studies highlight the invasive nature of this kind of probes. Specifically, Muzzio et al. (2003) compared three different types of traditional thief samplers with a new probe called *core sampler* (CS). It is an *end-sampling probe* which simply consists of a cylindrical tube, one end of which is tapered to a sharp angle (Fig. 1).

The sample is collected by inserting the CS into the powder bed to a predetermined depth, thus isolating a cylindrical core of powder in the tube. The core is then extracted by the action of a piston inserted into the tube. The final extraction operation requires a dedicated apparatus to be properly performed since it may need the application of large forces to push out the sample from the sampling tube. Despite its simplicity, the CS appears to be the best probe among those examined since it minimizes the drag of powder on the outer side of the probe; this means it does not cause disruption of the original structure of the bed of powder it is inserted in. External drag is caused because traditional thief probes are intrinsically intrusive. Since probes occupy a finite volume their insertion determines an equivalent displacement of material and the friction with the walls of the probe allows the transmission of stresses to the surrounding powder, generating shear. With the CS such powder displacement is minimized. Also internal drag results minimized (Muzzio et al., 2003).

Starting from these evidences on the advantages of CS, we deepened the features and applicability of CS-type probes, eventually suggesting a novel probe geometry. We collected evidences that a simple CS probe, even if it reduces drag, can induce relevant deformation of the sampled core thus biasing the measurement. We also explained this experimental evidence through powder mechanics arguments; we experimentally and theoretically demonstrated that CS can significantly compact the powder bed during insertion up to the point that the probe becomes blocked and cannot be completely filled. Consequently, we proposed an alternative probe, called *sliding cover sampler* (SCS) which was able to overcome these limitations giving better results than the CS.

2. Materials and methods

2.1. The sliding cover sampler (SCS)

In order to overcome some of the limitations of traditional sampling probes and to expand further the benefit introduced by the CS, it appeared important to improve the sampling procedure during the probe filling and the sample withdrawal stages. It seemed indeed important to reduce the undesired increase of stresses in the sampled powder, which eventually lead to compaction, incomplete probe filling and drag of material along the inner wall surface. It appeared likewise important to preserve the arching mechanism in the material during extraction, to allow the withdrawal of the probe with its sample without the need of closing the bottom of the probe. The addition of any end closure mechanism would indeed complicate the sampling procedure as well as being intrusive. All these motivations culminated in designing thief probes made of two parts, to be used at different times, in order to reduce the stresses on the powder during the probe insertion stage. It was made of a slide and a cover which needed to be inserted sequentially into the bed of powder to gather the sample. Also the extraction of the sample from the probe for subsequent analysis is much simpler, faster and more reliable. The concept is illustrated in Fig. 2, showing one of the possible geometries for the SCS.

This new thief probe can be considered as an evolution of the former CS. With respect to traditional probes, the underlying idea in CS and SCS is reversing the filling mechanism: it is not the powder that moves, entering into the probe cavities, but it is the probe that moves, enveloping a static portion of the powder bed, eventually isolating the sample from the bulk. Dealing with a static portion of powder has the advantage of eliminating segregation typical of flow conditions. The procedure of using the SCS consists of first inserting the slide into the powder bed until it reaches the predetermined sampling depth and then closing the probe with the sliding cover to isolate the core from the bulk. Once extracted, the probe provides the whole composition profile along the sampled bed with a single sampling operation. Differently from the CS sampling procedure, the sequential insertion of two independent parts dramatically reduces radial and axial stresses on the sample thus reducing further drag and compaction as will be clearer in the upcoming section.

Prototypes of the SCS were made with aluminum sheets (0.6 mm thin) but other materials would fit the scope such as stainless steel or rigid polymers, including Teflon-coated metals, with the purpose of tuning both the mechanical strength and the surface properties. Two different shapes were tested; a triangular and a semi-circular cross-section (see Fig. 3). In the *triangular* SCS the probe once closed has a triangular cross-section; slide and covers are indicated in Fig. 3a. Three sizes of the triangular SCS have been tested, with $L = 10$, 15 and 20 mm.

The *semi-circular* SCS is similar to the former excepted for the cover which is replaced by a semi-circular shell (Fig. 3b) in order to eliminate one angle and increase up to 90° the two acute angles on the side of the triangular SCS slide. This geometry was used to assess the effect of corners on powder drag. Corners are required to couple the two parts, but reproduce locally a narrow confinement where stress may increase. Two semi-circular SCSs have been designed, with $D = 8$ and 10 mm.

Once the mixture was sampled the extraction of the sample from the probe was much simpler, faster and more reliable with the SCSs than with the CS. As shown in Fig. 4, the probe was placed horizontally and the slide removed.

Fig. 2. (a) Picture of the SCS and (b) sketch of the components and operation.

In order to detach the sampled core from the slide before removal, thus preventing further drag and eliminating residual stresses, the slide was gently tapped. During this operation the sample did not move therefore preserving its structure. The sampled core then could be further sub-sampled by slicing it at the desired depth and with the desired size. This very simple procedure circumvented completely the limitations of extracting the sampled core by pushing it with a piston as required by CS.

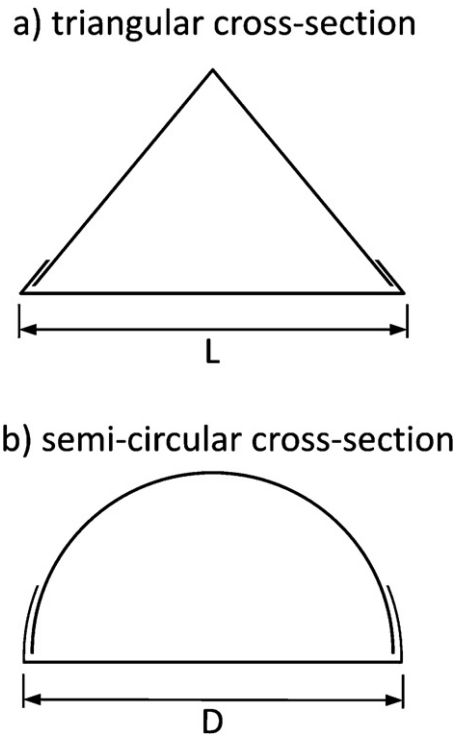

Fig. 3. Sketches of the SCS cross-sections used in this work, with their characteristic dimension. The slide is always the lower part and the cover above.

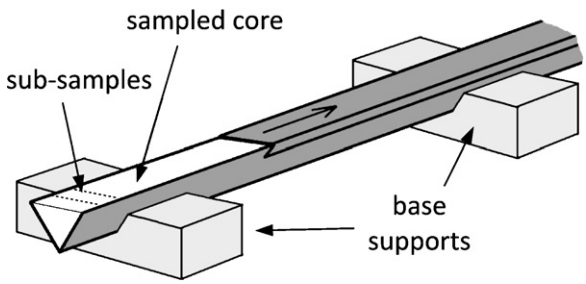

Fig. 4. Schematic of the procedure for unloading the SCS.

2.2. The sampling efficiency

In order to characterize and compare the performances of the different probes, a measure of sampling efficiency was proposed. It quantifies the compaction resulting from the insertion of the probe into the bed of powder. The efficiency was simply given by the ratio between the powder volume withdrawn by the probe, V_e, and the volume that could be theoretically withdrawn in the absence of friction and compaction, V_t. Because of the constant section of the probes, the efficiency reduced to the ratio between the length of the sampled core, h_e, and the depth of insertion, h_t:

$$\zeta = \frac{h_e}{h_t} \quad (1)$$

The efficiency was evaluated for any type and size of probes with lactose monohydrate (d_{90} = 72 μm) in a powder bed that was 150 mm deep. Larger bed thickness could be sampled with CS and SCS, however this depth was sufficient to highlight the differences in performance between the two probes. To minimize the powder compaction level prior to any sampling test, the bed of powder was created by pouring lactose through a sieve (Santomaso et al., 2003).

2.3. The drag test

The drag of material along the wall of the probe is caused by friction, which determines some shear in the neighboring material. If large, it can affect the significance of the sampled material. Friction is very significant for traditional probes and still present for both CS and SCS, although greatly reduced by the SCS strategy. To investigate the phenomenon, a powder bed with a depth of 80 mm was formed. It was made of materials with clearly contrasting colors, i.e. two layers of lactose monohydrate (white) separated by a layer of cocoa (dark) powders (d_{90} = 100 μm). The thickness of the upper layer was 20 mm and it was 30 mm for the others. To measure the magnitude of internal drag after insertion, a solidification technique was applied to the whole bed of powder with the probe inserted. Details of the technique can be found in Dal Grande et al. (2008) and is described in brief here. The technique requires wetting the powder with a liquefied mixture of hydrocarbons (Createc® Gmbh, Weiler Bremenried, Germany) at 80 °C (the melting point of the gel is 68 °C). The powders were impregnated by the gel both outside and inside the probe. After cooling at ambient temperature the bed of powder and the sample within the probe solidify. The probe was then removed and opened and the solidified core was transversally sectioned in slices 2 mm thick. This procedure gave, therefore, a spatial resolution of 2 mm which is higher than that of previous published works (order of 1 cm) and allowed to quantify the drag of the dark cocoa on the white lactose by image

analysis. A Matlab routine for image analysis was used to determine the average composition from digital images of each cross sectional slice. The composition was defined as the ratio between the number of dark pixels and the number of pixels of the total cross-sectional area. It was assumed that the cross-section with a cocoa composition equal to 50% could denote the initial interface between white lactose and dark cocoa powders. Composition values of the dragged material were measured up to an axial distance of 40 mm, that is, the value corresponding to the thickness of lactose layer. Each sampling experiment was replicated three times. The freezing procedure was used only in the drag test just to measure the spatial composition by image analysis and it is not necessary during normal sampling operations.

3. Results and discussion

Since SCS is expected to be an improvement of CS, the latter has been characterized first. In order to understand the major limitation of the CS, i.e. possibility of withdrawing non-representative samples, a brief description of the sampling procedure under the light of powder mechanics is required.

3.1. Powder mechanics

Three critical stages can be found during the sampling procedure with the CS: (a) probe filling during the insertion into the bed of powder, (b) probe withdrawal from the bed of powder and (c) probe emptying with the extraction of the sampled material. The first and the last stages are critical because of the high consolidation stresses which may develop in the material and will be examined in detail. The main physical assumptions and the underlying mathematics are similar to that of Janssen's original analysis of stresses in cylindrical bins and belong to classical powder mechanics (Brown and Richards, 1970; Nedderman, 1992; Schulze, 2008). As in Janssen's original analysis, the following assumptions have been made:

1. the material was assumed to be cohesionless. Cohesion would just complicate the analysis without giving further physical insight on stress transmission;
2. the stresses were assumed to act uniformly across any axial section of the material;
3. the axial and radial stresses were assumed to be principal stresses. This means that no shear stresses act axially and radially inside the material. In this case the relationship between the principal stresses is: $\sigma_{rr} = K\sigma_{zz}$ where σ_{rr} and σ_{zz} are the radial (or normal) and axial stresses, respectively, and K is a material constant also called Rankine coefficient or Janssen coefficient.
4. The bulk density was considered constant.

Differently from Janssen's analysis a further two assumptions were made:

5. gravity was neglected. Samples are small and so the gravitational contribution is negligible with respect to the frictional contribution developed by the walls of the probe. Moreover this assumption is compatible with the fact that sampling does not depend on the direction of probe insertion; the probe can be inserted in any direction (also horizontally) into the bed of powder;
6. the shear stress at the wall depends both on friction and adhesion so that the wall yield criterion follows a Coulomb-type relationship: $\tau_w = \mu_w\sigma_{rr} + a_w$ where τ_w is the shear stress at the wall, μ_w is the wall friction coefficient and a_w is the adhesion stress between the powder and the wall, which is present also in the absence of normal stresses σ_{rr}.

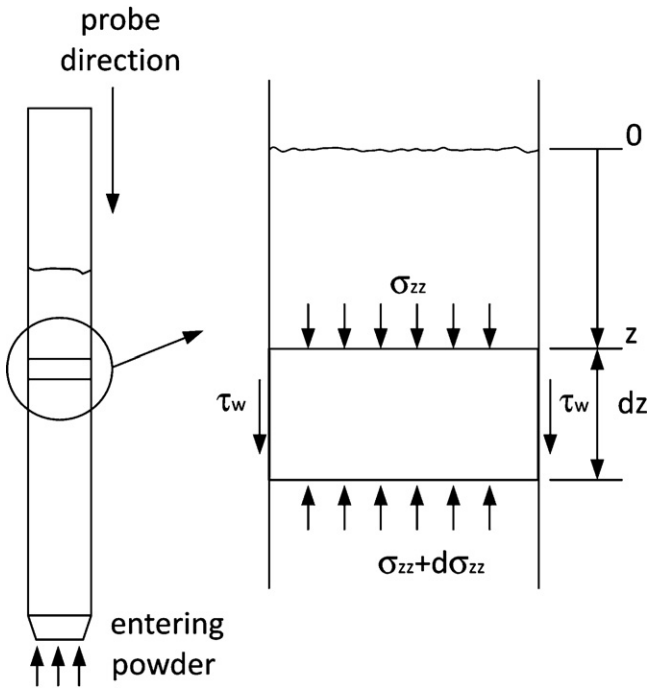

Fig. 5. Schematic of the core sampler with stresses on a differential element of powder during filling.

Similarly to Janssen's model, we do not consider the cohesion within the material (at particle-particle contacts), however we introduce cohesion between powder and wall through the adhesion term.

3.1.1. Core sampler filling

While inserting a cylindrical CS probe into a static bed of powder, the material inside the tube is (1) pushed inward by the new material entering at the bottom and (2) is constrained by wall friction.

The following force balance on a differential slice of material inside the tube (Fig. 5) holds:

$$\sigma_{zz}A + \tau_w P dz + (\sigma_{zz} + d\sigma_{zz})A \tag{2}$$

where A ($=\pi D^2/4$) and P ($=\pi D$) are the internal cross sectional area and the perimeter of the probe respectively. τ_w is the only external stress acting on the material since gravity has been discarded, hypothesis (4), and its direction is reversed with respect to that of Janssen's analysis since powder is moving in opposite direction with respect to the wall displacement, in this case. The following simple equation results:

$$\frac{d\sigma_{zz}}{dz} = \frac{4}{D}\tau_w$$

which gives the following simple first order non-homogeneous differential equation, considering hypotheses (3) and (6):

$$\frac{d\sigma_{zz}}{dz} - \frac{4}{D}\mu_w K\sigma_{zz} = \frac{4}{D}a_w \tag{3}$$

Integrated with the boundary condition:

$$\sigma_{zz} = 0 \quad \text{at } z = 0$$

gives

$$\sigma_{zz} = \frac{a_w}{\mu_w K}(e^{(4\mu_w K/D)z} - 1) \tag{4}$$

Eq. (4) shows that the axial stress that must be overcome to keep filling the probe grows exponentially with its filling level, z. For a

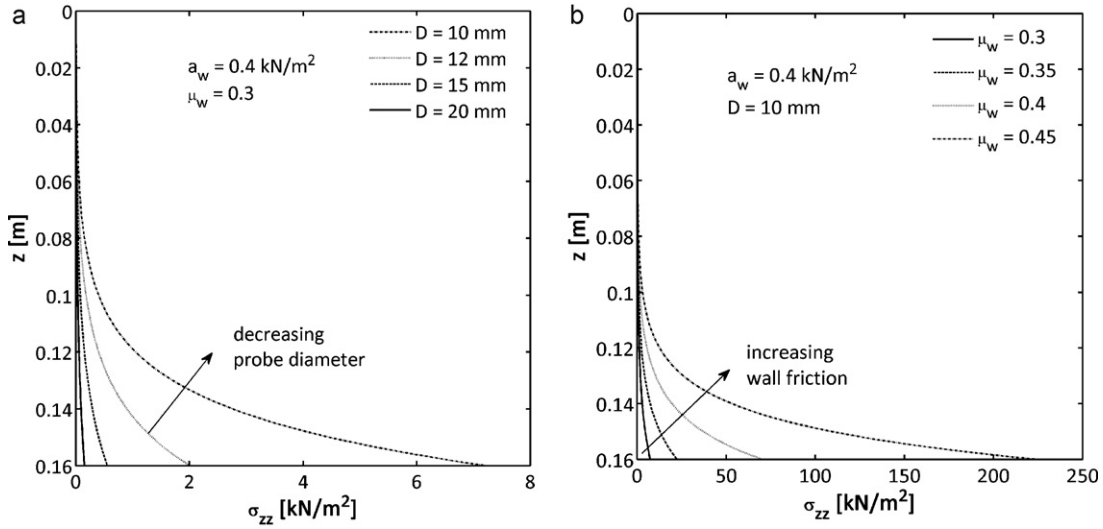

Fig. 6. Increase of vertical stress at the inlet of the *core sampler* as a function of the level of filling of the probe. (a) Effect of probe diameter and (b) of wall friction. K is assumed to be 0.4.

given final length of the sample H inside the probe, the consolidation stress at the inlet is:

$$\sigma_{zz}(H) = \frac{a_w}{\mu_w K}(e^{(4\mu_w K/D)H} - 1) \quad (5)$$

The stress developed does not depend on gravity but on the adhesive and frictional property of the wall (a_w, μ_w). Predictions of $\sigma_{zz}(z)$ are reported in Fig. 6 as a function of probe diameter, given μ_w, and the reverse. According to hypotheses (3) and (6), the radial and shear stresses at the walls increase with the same exponential trend. These stress profiles suggest that increasing drag at the walls (due to radial stresses, σ_{rr}) and powder compression (due axial stresses, σ_{zz}) have to be expected as a consequence of the progressive insertion (i.e. filling) of the probe. The level of drag and of consolidation should be greatest at the inlet and decrease along the probe, up to total extinction.

Fig. 6 shows also that combinations of probe size and surface finishing (or construction material), i.e. D and μ_w (typically small D and high μ_w), can easily increase stresses by one or two orders of magnitude. Consequently, each combination of probe diameter and surface finishing can lead to a critical amount of powder that can enter into the probe, before plugging it completely, so that no additional powder can be sampled.

According to Janssen's original analysis (Nedderman, 1992), the asymptotic (maximum) stress developed because of gravitational force would be:

$$\sigma_{zz}^{\infty} = \frac{\rho g D}{4\mu_w K}$$

Assuming $K = 0.4$; $\mu_w = 0.4$, $D = 10^{-2}$ m and $\rho = 400\,\mathrm{kg\,m^{-3}}$ (lactose), σ_{zz}^{∞} is $0.061\,\mathrm{kN\,m^{-2}}$, much smaller than stresses developed by frictional forces at the wall (see Fig. 6) and therefore fully justify hypothesis (5).

3.1.2. Core sampler extraction

After the filling of the CS probe, the powder remains consolidated and most of the stresses leading to the formation of the plug cannot be recovered unless the powder is sheared. While this allows the safe removal of the sample, without closing the probe extremity, complications do arise when recovering the sampled powder, since consolidation prevents any motion of the material and a piston is required to push out the plugged material (Muzzio et al., 1999, 2003).

3.1.3. Sample withdrawal from the CS

The use of a piston for sample extraction results in a uniaxial compression of a preconsolidated material. It can be treated within the same mathematical framework, but the direction of z is reversed with respect to the probe wall, since the material moves in the opposite direction and the boundary condition at the probe extremity is different.

The force balance gives the same expression as shown in Eq. (3). The pressure required to push out the sampled powder needs to overcome the stresses developed at the walls by the consolidated material. If it is assumed that the maximum consolidation stress gained during the filling stage, $\sigma_{zz}(H)$, persists during the withdrawal stage, it can be modeled as an overload, $Q_0 = \sigma_{zz}(H)$, acting on the surface and opposing the action of the piston (Fig. 7).

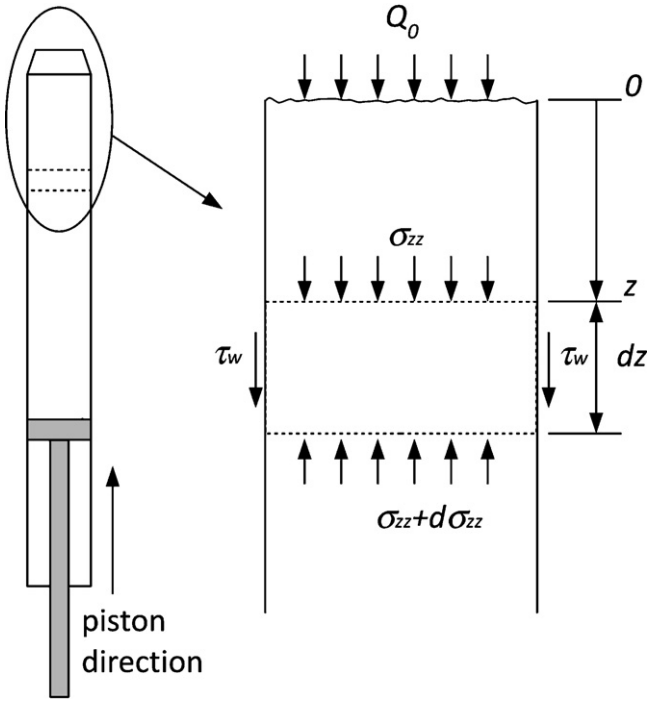

Fig. 7. Schematic of the core sampler with stresses on a differential element of powder during sample extraction with a piston.

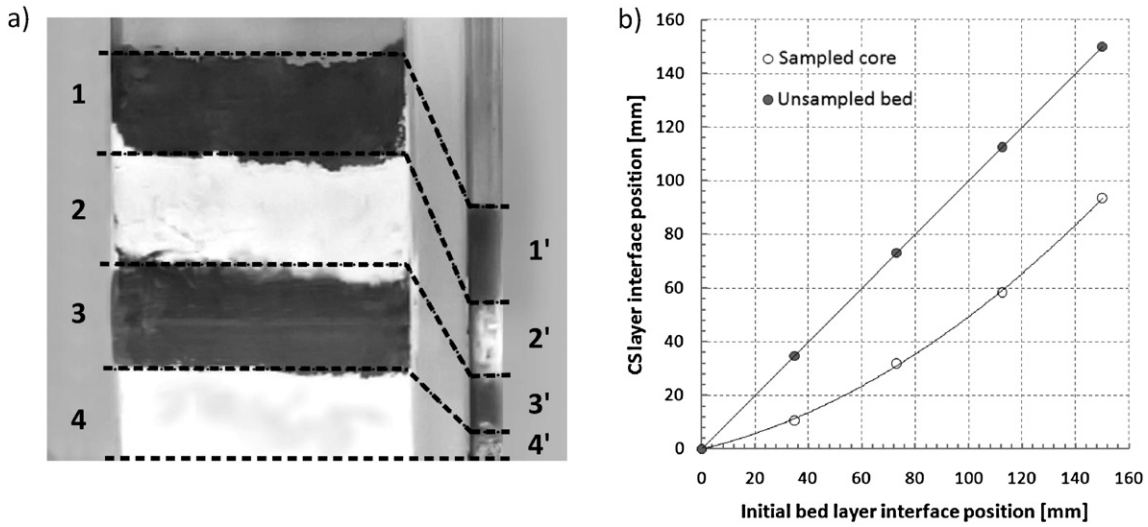

Fig. 8. Qualitative and quantitative comparison of bed structure before and after sampling with a glass core sampler.

The overload acting at the probe extremity is given by Eq. (5). Therefore using it as a new boundary condition:

$$\sigma_{zz}(H) = Q_0 = \frac{a_w}{\mu_w K} e^{(4\mu_w K/D)H} - 1 \quad \text{at } z = 0$$

Integration of Eq. (3) gives:

$$\sigma_{zz} = \frac{a_w}{\mu_w K}[e^{(4\mu_w K/D)(z+H)} - 1] \tag{6}$$

Since the height z of the plug to be pushed out is identical to H, the axial stress which has to be transferred through the piston to push the plug results in an exponent that is double with respect to that of Q_0 in Eq. (5). This means that stresses during sample withdrawal can increase by many orders of magnitude with respect to those developed during probe filling. This obviously would further compact the sample, generating strong shear stresses at the wall, according to hypotheses (3) and (6), and forcing an unpractical procedure to withdraw the sample (Muzzio et al., 1999).

3.2. Experiments

Before investigating the advantages of the SCS probes, the effects of stress distribution and the extent of compaction of the materials inside the CS probe have been experimentally evaluated. A bed of powder with a total depth of 150 mm was prepared with four layers of equal thickness of monohydrate lactose and cocoa powder (dark), as shown in Fig. 8.

The CS is in this case a transparent glass tube (i.d. 15 mm and o.d. 18 mm), which was vertically introduced into the stratified bed. The structure of the sample withdrawn by the glass probe was then compared to the structure of the original bed. Fig. 8a clearly shows the level of compaction caused by this thief probe. Specifically, we observe:

- The height of the sample is on the whole reduced by a 40%. Sampling efficiency as defined in Eq. (1) is: $\zeta = 60\%$.
- The deformation of the bands is not linear with the depth (Fig. 8b). The bottom lactose layer is strongly compressed confirming the formation of the plug while the upper cocoa layer is almost uncompressed.
- Drag on the inner walls of the probe can be deduced by the progressive darkening of the white bands (Fig. 8a).
- Drag increases with the level of compaction (in particular with radial stresses at the walls).

Table 1
Measured sampling efficiency.

Type of SCS	ζ [%]	Std. dev.
Core sampler, $D = 15$ mm	60	1.67
Triangular, $L = 10$ mm	85	0.77
Triangular, $L = 15$ mm	86	1.76
Triangular, $L = 20$ mm	87	0.77
Semi-circular, $D = 8$ mm	89	1.02
Semi-circular, $D = 10$ mm	95	0.67

3.3. The sampling efficiency measurements

Table 1 shows the sampling efficiency obtained by the SCSs on the 150 mm thick lactose bed. Results are the average of three tests for each thief probe. The efficiency of the glass CS is also reported, for comparison.

As initially expected, the sampling efficiency increases significantly with the new SCS probes, the most efficient being the largest semi-cylindrical. Results confirm that the new probes lead to a lower powder consolidation when inserted into the bed, thus preventing the formation of a plug.

To quantify the extent of compaction of the materials inside the SCSs, the variation of bulk density of the material contained into the probe has been measured by weighting subsamples of a given volume. Experiments were carried out on powder beds of monohydrate lactose, 150 mm deep. After sampling with the SCSs, the core collected was transversally sectioned with a resolution of 10 mm along the probe; each portion of the core was weighed and the bulk density calculated.

The axial profile of density inside each probe is shown in Fig. 9. A comparison with the calculated density inside the CS is also shown. The density for CS was estimated using the information from Fig. 8 on the level of sample compression. The differences of levels between the lactose–cocoa interfaces allowed the degree of compression of the sample to be estimated and therefore, the increase in bulk density. So only four data, estimated from the thickness of the four alternating layers were available. However, it is clear that the material is much more consolidated in the case of the CS, as a consequence of the exponential increase of the consolidation stresses. For the SCSs, these wider probes correspond to lower compaction according to the model predictions. At comparable size, the semi-cylindrical probes yield the lowest bulk densities confirming the above results on sampling efficiency.

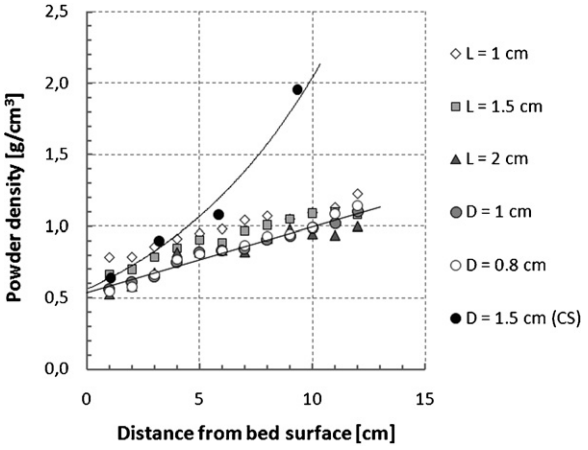

Fig. 9. Axial bulk density trends in SCS and CS after sampling.

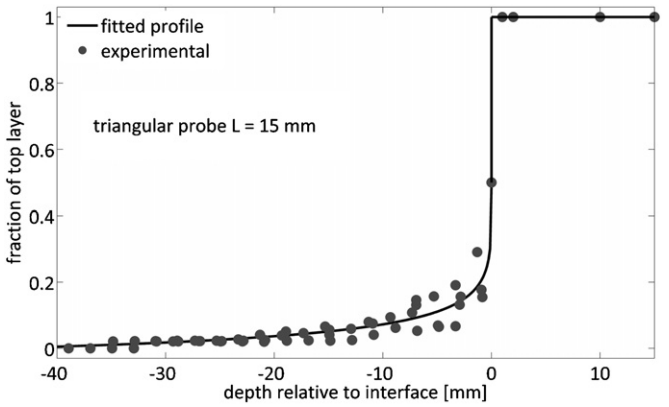

Fig. 11. Composition profile of cocoa powder (top layer) as a function of distance from the cocoa–lactose interface.

3.4. The drag characterization

The intensity of material drag during probe insertion has been evaluated for the two SCS shapes. A sharp material interface and the solidification and slicing technique described above have been used.

Fig. 10 shows typical results, with three cross-sections extracted from the solidified core of a triangular (L = 20 mm) and a semi-cylindrical (D = 10 mm) SCS. Sections are progressively farther from the cocoa(dark)–lactose(white) interface, illustrating the carryover of dark powder in the white region.

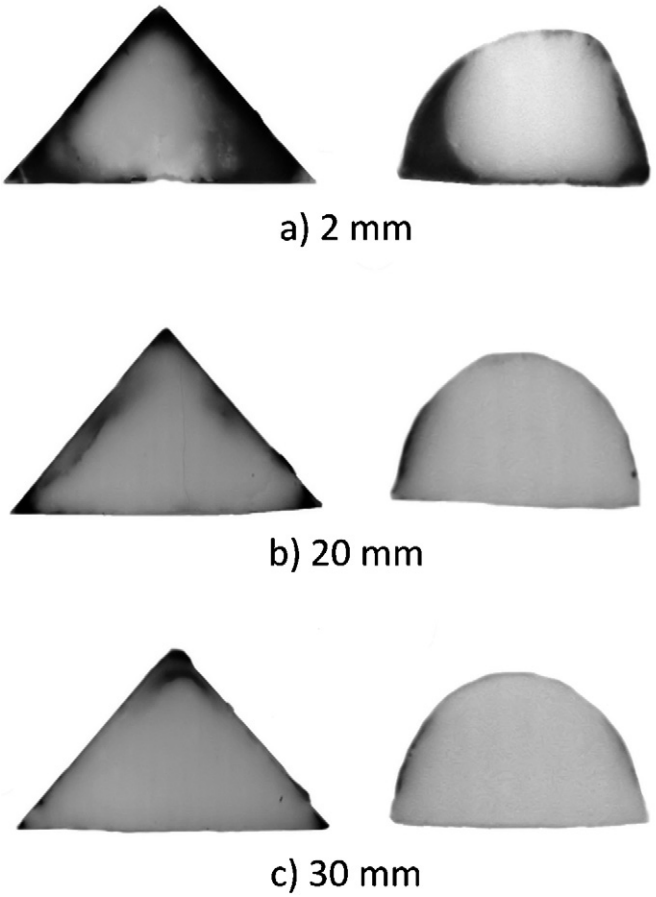

Fig. 10. Cross-sectional view at 3 different distances (2, 20, 30 mm) below the cocoa–lactose interface for a triangular (L = 20 mm) and a semi-cylindrical (D = 10 mm) probe. Sections are not represented at the same scale.

It is perceived that the semi-cylindrical probe reduces drag with respect to the triangular probe, due to reduced amount of dark powder being dragged to the lactose area. Repeated experiments confirmed that drag in the triangular probe is more intense at the corners, as apparent form (Fig. 10). Friction in narrower confinements (acute angle corners) is higher, presumably because of a larger local stress, eventually leading to significant drag. On the contrary, the semi-cylindrical construction reduces narrow angles and thus material drag, suggesting that an even better SCS would be obtained by two semi-cylindrical parts, which are suitably coupled.

The same freezing and slicing technique followed by image analysis allowed for a quantitative analysis of the penetration of contamination across a sharp composition interface, due to material drag. The experimental composition profile expressed as fraction of top material (cocoa powder) versus the depth relative to the interface between the two materials is shown in Fig. 11 for a triangular SCS (L = 15 mm). An interpolation curve is superimposed, to allow an easier comparison among several data.

Fig. 11 shows that the amount of top material dragged below the interface drops rapidly, while there is no mutual contamination of the two powders above the interface, because of the direction of insertion. The extraction procedure for the SCS does not require the powder to move further, since the core is simply accessed by removing the slide. Consequently, no additional upwards contamination by drag is possible and the composition profile above the interface coincides with what is expected.

To compare the effect of the two different geometries (semi-circular and triangular cross section) two probes with the same width (i.e. those with the slide 10 mm wide) have been compared. Similar to Fig. 11, Fig. 12 compares the composition profiles of a triangular and a semi-circular probe below the lactose–cocoa interface. The two probes behave similarly, though the semi-circular ones has a faster decay of powder concentration from the top layer (i.e. less powder drag after insertion) with respect to the triangular one. That was expected because of the reduction of narrow corners. Table 2 compares the contamination due to material drag at the walls for all the probes. The SCS results are also compared with available Literature data for other thief probes in terms of fraction of top material at a distance of 10 mm below the interface.

On the whole, the present data for SCS are comparable, frequently better, than CS, according to the Literature measurements, with exception of a very narrow (10 mm wide) triangular probe. Further SCS and CS performances are clearly superior to other thief probes, including commercial ones. It is worth observing that the comparison between concentration at a given distance below the

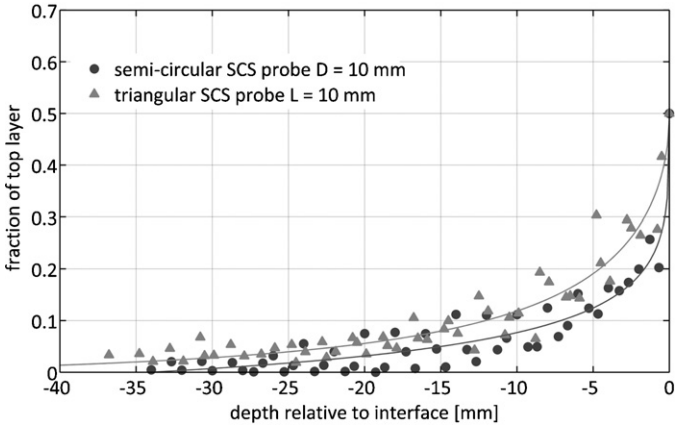

Fig. 12. Composition profile of cocoa powder (top layer) as a function of distance from the cocoa–lactose interface, comparing two geometries: semi-circular and triangular cross-section.

Table 2
Drag efficiency as % of material above the interface found 10 mm below it.

Type of sampler	References	Composition (%)
SCS (*L* = 10 mm)	Present work	12
SCS (*L* = 15 mm)	Present work	6
SCS (*L* = 20 mm)	Present work	6
SCS (*D* = 8 mm)	Present work	6
SCS (*D* = 10 mm)	Present work	8
Core sampler	Muzzio et al. (1999, 2003)	<10
Slug (*end-sampler*)	Muzzio et al. (1999)	45
Side sampler	Muzzio et al. (1999, 2003)	90

surface is also negatively biased by the high level of consolidation (and therefore compression) of the sample in the CS case. Moreover the core withdrawal procedure required by the CS may introduce additional errors, in the form of reverse drag. Contamination of the upper layer by materials in the lower ones can be generated by the inversion of the material translation within the probe, required by CS for core extraction. Such biases are not present in the procedure for SCS core extraction.

4. Conclusions

In this paper novel thief probes have been conceived, designed and characterized for cohesive powders, here referred to as the sliding cover samplers (SCS). They consist of two thin metallic shells to be inserted sequentially into the bed of powder in order to extract a representative core. Due to the thin profile of the shells and of the particular insertion procedure, stresses on the powder are minimized, which reduces both the invasiveness on the bed and the dragging of material in the sample. The extremity of the probe does not require to be closed since cohesion prevents the outflow of material from the probe during the extraction. The advantage of this sampling probes is that powder does not move to enter the probe but it is the probe that envelopes a static portion of material. Also the final withdrawal of the core from the probe does not require the powder to move since it is the probe that is opened, exposing the sampled core. This procedure reduces the possibility of segregation (which is associated to flow conditions) and minimizes the possibility of contaminating the sample with material dragged from the upper levels, as quantitatively proved in this work. SCSs of different shapes and sizes have been tested and compared with other kinds of thief probes (commercial and not) and the results showed that SCSs are more efficient than traditional devices since they significantly reduce both the consolidation and the drag of the powder. SCSs probes are not limited to any sampling depth, differently from CS. SCS probes also allow in a single operation to determine a composition profile along the whole powder bed depth. Considering that SCSs simplify the probe design and use, they can be considered a viable alternative to commercial thief probes when dealing with cohesive powders.

References

Benedetti, C., Abatzoglou, N., Simard, J.-S., McDermott, L., Léonard, G., Cartilier, L., 2007. Cohesive, multicomponent, dense powder flow characterization by NIR. Int. J. Pharm. 336, 292–301.
Bridgwater, J., 1976. Fundamental powder mixing mechanisms. Powder Technol. 15, 215–236.
Brown, R.C., Richards, J.C., 1970. Principles of Powder Mechanics. Pergamon.
Dal Grande, F., Santomaso, A., Canu, P., 2008. Improving local composition measurements of binary mixtures by image analysis. Powder Technol. 187, 205–213.
Danckwerts, P.V., 1953. Theory of mixtures and mixing. Chem. Eng. Res. 6, 355.
Harnby, N., 1992. The mixing of cohesive powders. In: Harnby, N., Edwards, M.F., Nienow, A.W. (Eds.), Mixing in the Process Industry. Butterworth-Heinemann, Oxford.
Harnby, N., 2000. An engineering view of pharmaceutical powder mixing. Pharm. Sci. Technol. Today 3, 303.
Mendez, A.S.L., de Carli, G., Garcia, C.V., 2010. Evaluation of powder mixing operation during batch production: application to operational qualification procedure in the pharmaceutical industry. Powder Technol. 198, 310–313.
Muzzio, F.J., Goodridge, C.L., Alexander, A., Arratia, P., Yang, H., Sudah, O., Mergen, G., 2003. Sampling and characterization of pharmaceutical powders and granular blends. Int. J. Pharm. 250, 51–64.
Muzzio, F.J., Robinson, P., Wightman, C., Brone, D., 1997. Sampling practices in powder blending. Int. J. Pharm. 155, 153–178.
Muzzio, F.J., Roddy, M., Brone, D., Alexander, A., Sudah, O., 1999. An improved powder-sampling tool. Pharm. Technol. 9, 92–100.
Nedderman, R.M., 1992. Statics and Kinematics of Granular Materials. Cambridge University Press, Cambridge.
Santomaso, A., Lazzaro, P., Canu, P., 2003. Powder flowability and density ratios: the impact of granules packing. Chem. Eng. Sci. 58, 2857–2874.
Santomaso, A., Olivi, M., Canu, P., 2004. Mechanisms of mixing of granular materials in drum mixers under rolling regime. Chem. Eng. Sci. 59, 3269–3280.
Santomaso, A., Olivi, M., Canu, P., 2005. Mixing kinetics of granular materials in drums operated in rolling and cataracting regime. Powder Technol. 152, 41–51.
Schulze, D., 2008. Powders and Bulk Solids: Behavior, Characterization, Storage and Flow. Springer-Verlag, Berlin, pp. 259–265.
U.S. Food and Drug Administration, 2003. Guidance for Industry, Powder Blends and Finished Dosage Units—Stratified In-Process Dosage. Unit Sampling and Assessment, Draft Guidance, Pharmaceutical CGMPs.
Zik, O., Levine, D., Lipson, S.G., Shtrikman, S., Stavans, J., 1994. Rotationally induced segregation of granular materials. Phys. Rev. Lett. 73, 644–647.